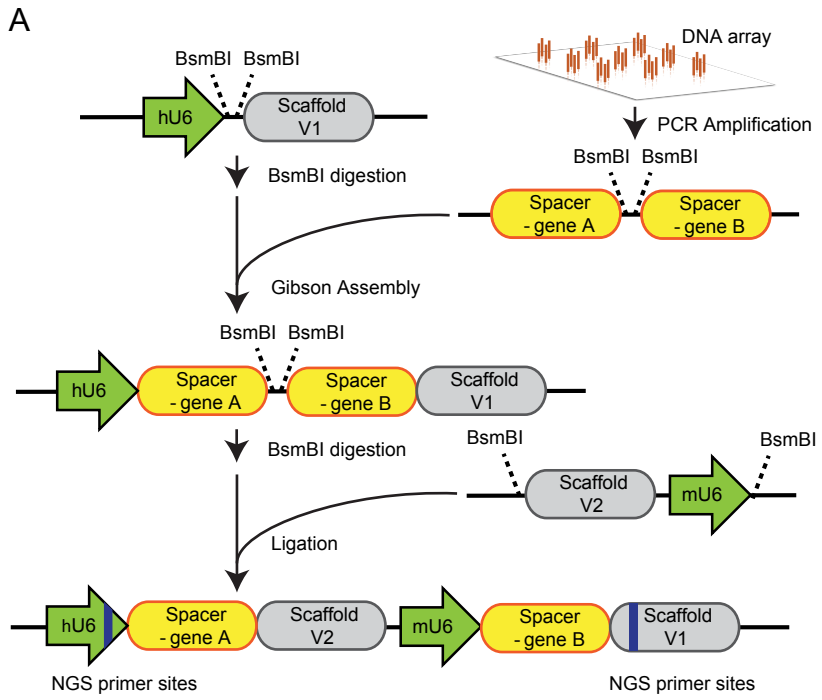
A
BsmBI BsmBI
hU6
Scaffold V1
DNA array
PCR Amplification
BsmBI digestion
BsmBI BsmBI
Spacer - gene A
Spacer - gene B
Gibson Assembly
BsmBI BsmBI
hU6
Spacer - gene A
Spacer - gene B
Scaffold V1
BsmBI digestion
BsmBI
BsmBI
Scaffold V2
mU6
Ligation
hU6
Spacer - gene A
Scaffold V2
mU6
Spacer - gene B
Scaffold V1
NGS primer sites
NGS primer sites

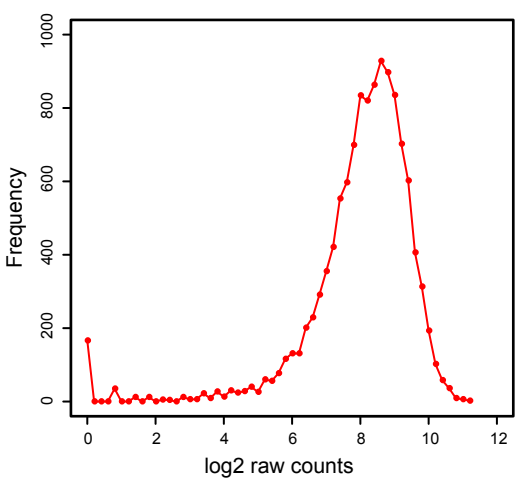
B
Frequency
0
200
400
600
800
1000
0
2
4
6
8
10
12
log2 raw counts

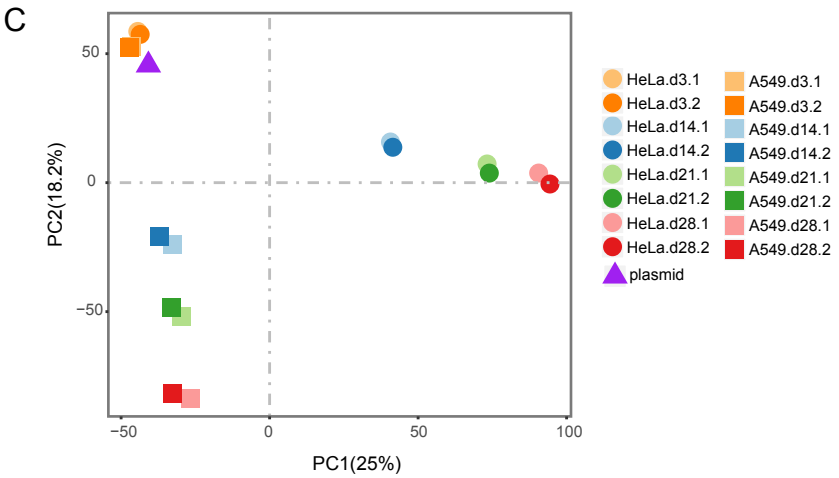
C
PC2(18.2%)
50
0
−50
−50
0
50
100
PC1(25%)
HeLa.d3.1
HeLa.d3.2
HeLa.d14.1
HeLa.d14.2
HeLa.d21.1
HeLa.d21.2
HeLa.d28.1
HeLa.d28.2
plasmid
A549.d3.1
A549.d3.2
A549.d14.1
A549.d14.2
A549.d21.1
A549.d21.2
A549.d28.1
A549.d28.2

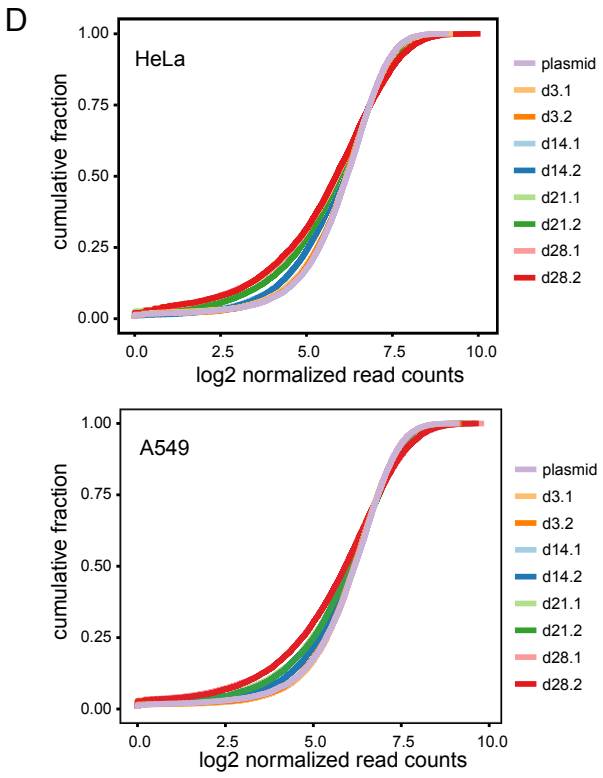
D
HeLa
cumulative fraction
1.00
0.75
0.50
0.25
0.00
0.0
2.5
5.0
7.5
10.0
log2 normalized read counts
plasmid
d3.1
d3.2
d14.1
d14.2
d21.1
d21.2
d28.1
d28.2
A549
cumulative fraction
1.00
0.75
0.50
0.25
0.00
0.0
2.5
5.0
7.5
10.0
log2 normalized read counts
plasmid
d3.1
d3.2
d14.1
d14.2
d21.1
d21.2
d28.1
d28.2

Figure S1.

Figure S1. Schematic of dual-gRNA-library construction and quality control of screens; related to Figure 1. (A) Oligonucleotides bearing two sgRNA spacers were synthesized, amplified, and cloned into a lentiviral gRNA cloning vector. Next, a fragment containing a sgRNA scaffold and the mouse U6 promoter was inserted between the two spacers to yield the final dual-gRNA expression construct. A pair of primer matching sites labeled in blue were designed for enrichment of the two spacer regions prior to deep sequencing analysis. (B) Frequency distribution of the metabolism dual-gRNA plasmid library. (C) Principle component analysis (PCA) of the dual-gRNA read count distributions. (D) Cumulative frequency of dual-gRNA constructs by deep sequencing. Shift in the curves at days 14, 21, and 28 represents the depletion of dual-gRNA constructs. Each time point was measured in duplicates.

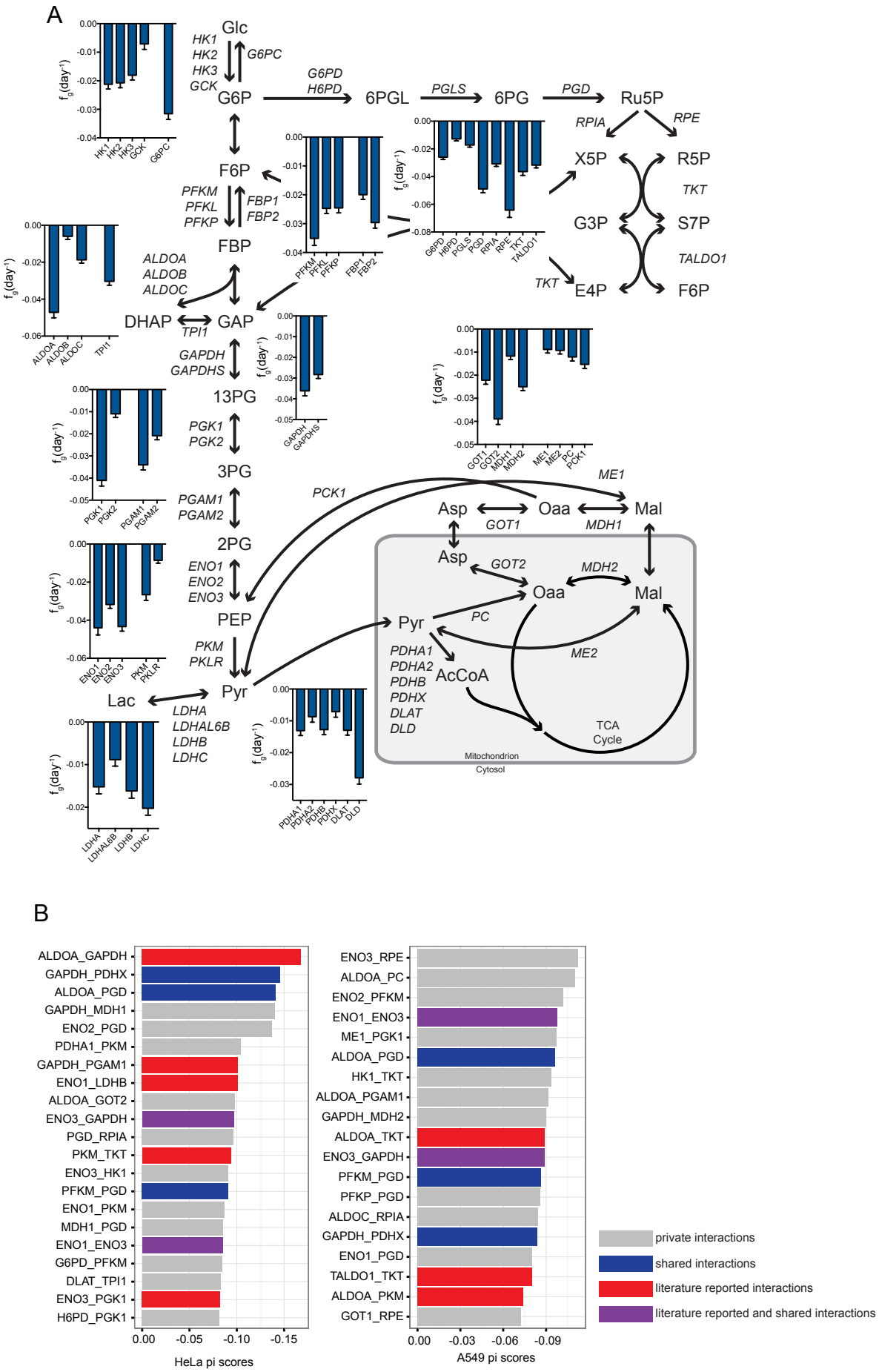
A
Glc
HK1
HK2
HK3
GCK
G6PC
G6P
G6PD
H6PD
6PGL
PGLS
6PG
PGD
Ru5P
RPIA
RPE
X5P
R5P
TKT
G3P
S7P
TALDO1
TKT
E4P
F6P
F6P
PFKM
PFKL
PFKP
FBP1
FBP2
FBP
ALDOA
ALDOB
ALDOC
DHAP
TPI1
GAP
GAPDH
GAPDHS
13PG
PGK1
PGK2
3PG
PGAM1
PGAM2
2PG
ENO1
ENO2
ENO3
PEP
PKM
PKLR
Pyr
Lac
LDHA
LDHAL6B
LDHB
LDHC
PCK1
ME1
Asp
Oaa
Mal
GOT1
MDH1
Asp
GOT2
MDH2
Oaa
Mal
Pyr
PC
ME2
PDHA1
PDHA2
PDHB
PDHX
DLAT
DLD
AcCoA
TCA
Cycle
Mitochondrion
Cytosol
B
ALDOA_GAPDH
GAPDH_PDHX
ALDOA_PGD
GAPDH_MDH1
ENO2_PGD
PDHA1_PKM
GAPDH_PGAM1
ENO1_LDHB
ALDOA_GOT2
ENO3_GAPDH
PGD_RPIA
PKM_TKT
ENO3_HK1
PFKM_PGD
ENO1_PKM
MDH1_PGD
ENO1_ENO3
G6PD_PFKM
DLAT_TPI1
ENO3_PGK1
H6PD_PGK1
0.00
-0.05
-0.10
-0.15
HeLa pi scores
ENO3_RPE
ALDOA_PC
ENO2_PFKM
ENO1_ENO3
ME1_PGK1
ALDOA_PGD
HK1_TKT
ALDOA_PGAM1
GAPDH_MDH2
ALDOA_TKT
ENO3_GAPDH
PFKM_PGD
PFKP_PGD
ALDOC_RPIA
GAPDH_PDHX
ENO1_PGD
TALDO1_TKT
ALDOA_PKM
GOT1_RPE
0.00
-0.03
-0.06
-0.09
A549 pi scores
private interactions
shared interactions
literature reported interactions
literature reported and shared interactions

Figure S2.

Figure S2. CRISPR screening results reveal metabolic network dependencies; related to Figure 2. (A) SKO fitness scores for A549 cells, plotted as f_g (day^{-1}), with a more negative score representing a decrease in fitness with SKO. Plotted as mean ± SD. (B) Gene pairs with significant genetic interaction scores (z-score < -3) are shown. Conserved interactions cross HeLa and A549 are indicated in blue. Previously reported interactions are indicated in red. Purple indicates the conserved interactions which have been previously reported.

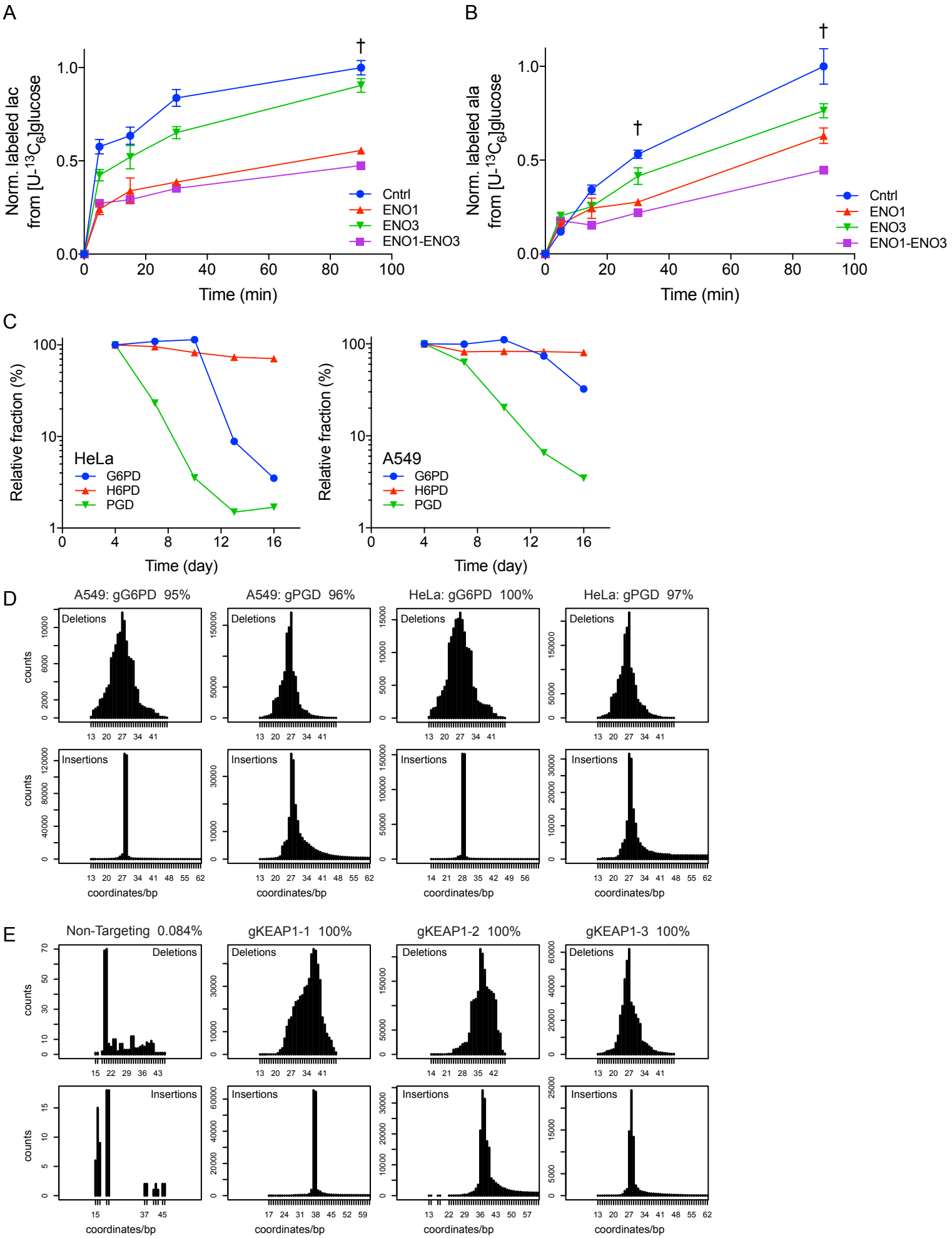
A
Norm. labeled lac from [U-13C6]glucose
Time (min)
Cntrl
ENO1
ENO3
ENO1-ENO3
†
B
Norm. labeled ala from [U-13C6]glucose
Time (min)
C
Relative fraction (%)
HeLa
G6PD
H6PD
PGD
Time (day)
A549
D
A549: gG6PD 95%
A549: gPGD 96%
HeLa: gG6PD 100%
HeLa: gPGD 97%
Deletions
Insertions
counts
coordinates/bp
E
Non-Targeting 0.084%
gKEAP1-1 100%
gKEAP1-2 100%
gKEAP1-3 100%

Figure S3.

Figure S3. Screening results validated through metabolic flux measurements and fitness assays; related to Figure 3. (A, B) Metabolic validation of DKO interaction in *ENO1/ENO3*. DKO significantly lowered flux through glycolysis over control or SKOs. A, measurement of labeled Lactate. B, measurement of labeled Alanine. † indicates statistical significance ($p<0.05$) for all conditions as compared to DKO. (C) SKO competition assay of oxPPP genes in HeLa (left) and A549 (right) cells. HeLa data replicated from Figure 3L and log transformed for comparison. (D) Deep sequencing analysis of indels (insertions and deletions) introduced by CRISPR-Cas9 at 10 days after transduction of *G6PD* or *PGD* gRNA constructs. (E) Deep sequencing analysis of indels introduced by CRISPR-Cas9 at two weeks after transduction of *KEAP1* gRNA constructs in HeLa cells. Ordinate shows the read counts of indels at each corresponding location. Most cells were successfully targeted after transduction of gRNAs, while only a background level of mutagenesis was observed in the cells transduced with non-targeting control gRNAs. These experiments suggest high targeting efficiency in both the A549 and HeLa Cas9-stable cell lines. (A-C) Plotted as mean ± SEM.

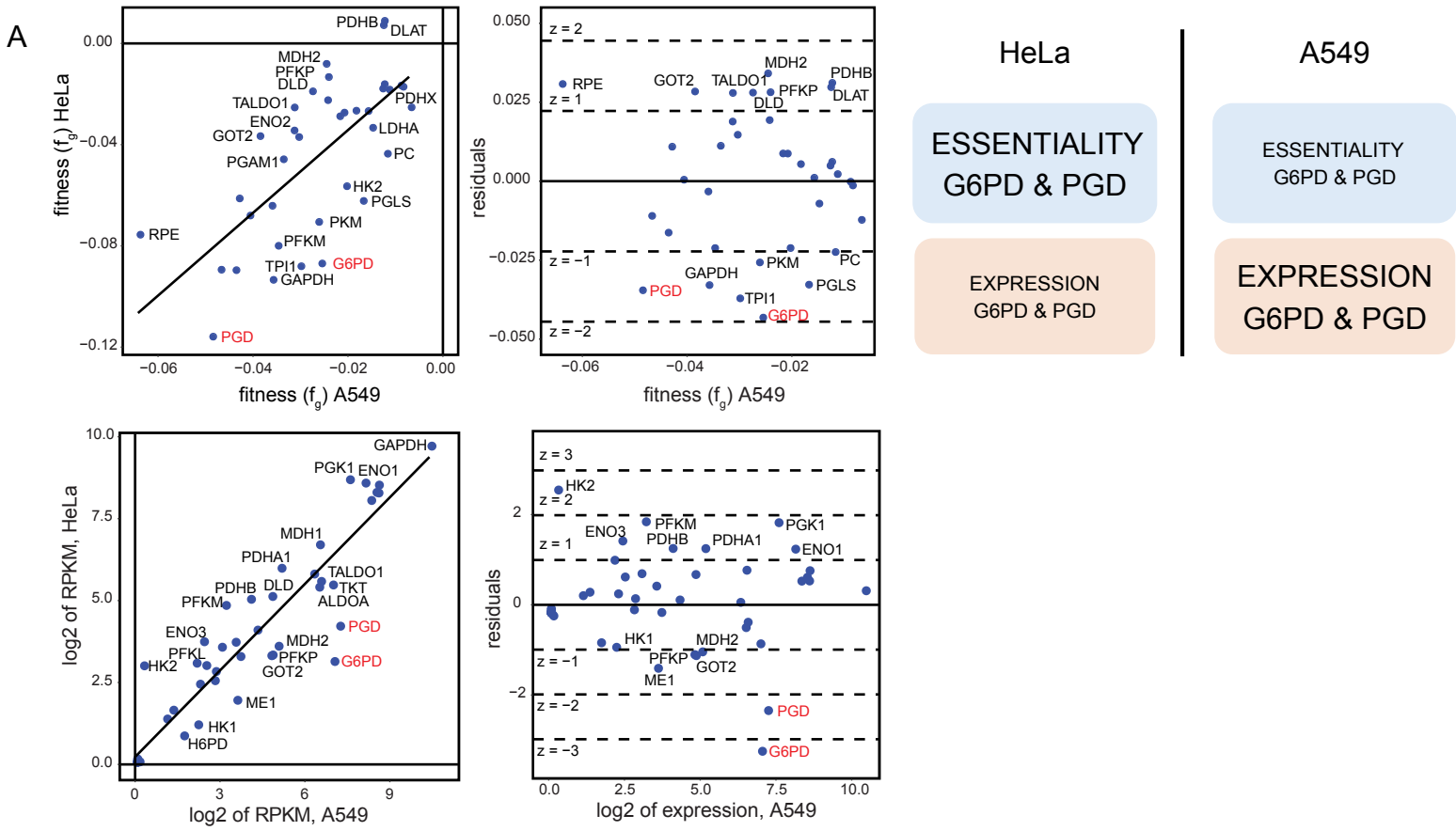

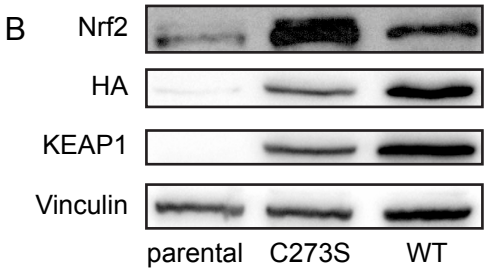

C

Step1: measure the fitness of reference cells

$$N_c(t_2) = N_c(t_1) \times 2^{(f_0 \times (t_2 - t_1))}$$

Step2: measure the fitness of gRNA in Keap mutation cells (slope)

$$\frac{N_{gRNA}(t_2)}{N_0(t_2)} = \frac{N_c(t_1) \times 2^{(f_0 + \Delta f_{gRNA})(t_2 - t_1)}}{N_0(t_1) \times 2^{(f_0)(t_2 - t_1)}}$$

Step3: calculate the relative effect of PGD knockout

$$R_{PGD,KEAP1} = \frac{(f_0 + \Delta f_{PGD,KEAP1}) - (f_0 + \Delta f_{NTC,KEAP1})}{f_0 + \Delta f_{NTC,KEAP1}}$$

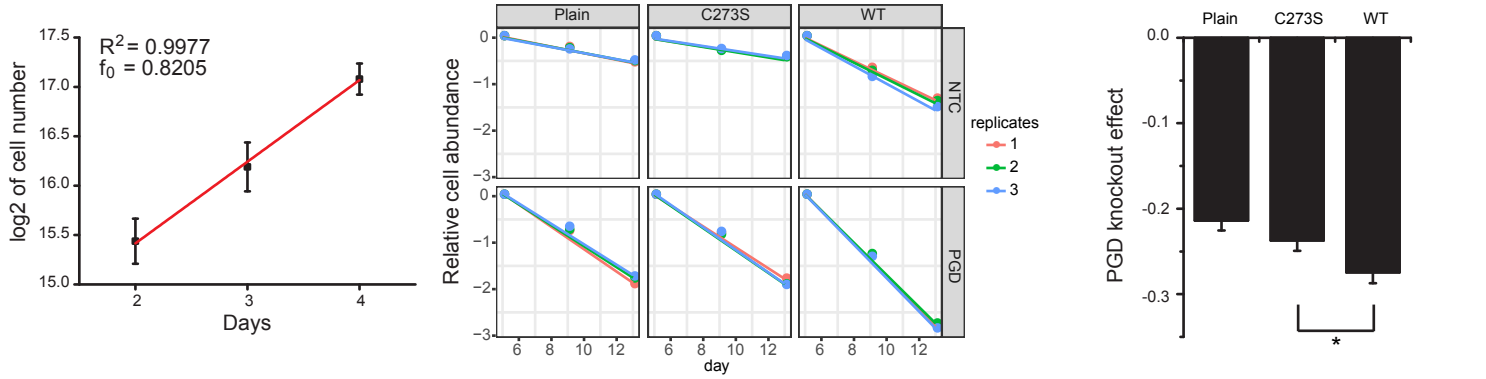

Figure S4.

Figure S4. *KEAP1* mutational status alters redox metabolism and impact of oxPPP gene knockouts on cellular fitness; related to Figure 4. (A) Scatter plots (left) of SKO fitness and gene expression in HeLa versus A549. Residual plots (right) of linear regressions showing the outliers between HeLa and A549. oxPPP genes (*G6PD* and *PGD*) showed more essentiality in HeLa cells versus A549, while their mRNA expression levels are lower in HeLa cells versus A549. (B) Immunoblot of A549s with *KEAP1* mutant panel. Superfluous lane (negative control) removed from image. (C) Measurement of relative *PGD* perturbation effect in A549 cells across *KEAP1* mutant panel. Growth curve of the reference cells, which is tdtomato+ cells in this case, and its absolute fitness (f_0) was extracted by counting average cell numbers in three independent experiments for three days. The fitness of *PGD* perturbation ($\Delta f_{PGD,KEAP1}$) relative to non-targeting controls (NTC) in *KEAP1* mutation cells were measured by competitive assay. Finally, by incorporating also the absolute fitness of reference cells, the relative effects of *PGD* perturbation ($R_{PGD,KEAP1}$) in *KEAP1* mutant cells was calculated.